Restart Expedites Quantum Walk Hitting Times

R. Yin and E. Barkai
Department of Physics, Institute of Nanotechnology and Advanced Materials, Bar-Ilan University, Ramat-Gan 52900, Israel

(Received 8 May 2022; accepted 22 December 2022; published 2 February 2023)

Classical first-passage times under restart are used in a wide variety of models, yet the quantum version of the problem still misses key concepts. We study the quantum hitting time with restart using a monitored quantum walk. The restart strategy eliminates the problem of dark states, i.e., cases where the particle evades detection, while maintaining the ballistic propagation which is important for a fast search. We find profound effects of quantum oscillations on the restart problem, namely, a type of instability of the mean detection time, and optimal restart times that form staircases, with sudden drops as the rate of sampling is modified. In the absence of restart and in the Zeno limit, the detection of the walker is not possible, and we examine how restart overcomes this well-known problem, showing that the optimal restart time becomes insensitive to the sampling period.

DOI: 10.1103/PhysRevLett.130.050802

Introduction.—First-passage processes are ubiquitous in practically all fields of science. Probably the simplest approach uses a random walker in search of a target, as found for diffusion-controlled reactions [1,2]. This common method does not demand an input of energy, however, it is nonefficient as the random walker resamples previously visited locations, and further, the walker, according to the laws of chance, may stray far from the target. In the context of biochemical reactions, nature found a way to overcome this problem, and that is with a restart strategy [3–6]. It turns out that, sometimes, if the search does not find its target, it is better to give up and start the process anew. Restarts were employed to accelerate algorithms [7,8], and then, considered in generality in the context of stochastic processes [9,10], rapidly encompassing various contexts including classical search theory, chemical physics, and population dynamics, etc. In this well-studied field, the basic questions are what are the nonequilibrium steady states emerging from restart, and what is the optimal time to restart [7–35]?

As the counterpart of classical random walks, quantum walks are widely applied in many different fields, ranging from transport in waveguides to ultracold atoms to light-harvesting dynamics in biochemistry [36–40], and therefore, rather naturally, a few previous works addressed the restart problem with an underlying quantum dynamics [41–47]. At the same time, quantum search and transport, in the absence of restarts, has an antagonist: the dark subspace [48,49] caused by destructive interference. This problem works against the quantum advantage of ballistic propagation [39], which can be useful for search. This means that, for quantum walks with dark states, the detection probability, defined below, is less than unity even for small systems. Overcoming this hurdle is important for efficient quantum search, and restarts are a powerful approach for that aim. However, one may not introduce restarts blindly, as the goal is not merely to get rid of the dark states, but rather to optimize the time for search. The basic questions are the following. How to choose the time for the restart so that the quantum search time is minimized? Will the ballistic superiority of the quantum search be retained when restart is added? What are the fundamental differences between quantum and classical restarts? To characterize the time for search, we utilize the concept of quantum hitting time, or the first-detected-passage time (FDPT). The model we consider is a tight-binding quantum walk with repeated monitoring, which was studied extensively in the absence of restart [49–58]. Such repeated monitoring or measurements have been implemented, for example, on IBM quantum computers [59]. Our Letter paves the way for the speedup of quantum hitting times, on quantum computers, which, as mentioned, is particularly important in the presence of dark states.

The benchmark model for classical restart is a diffusive particle whose position is reset at some random time t_r [9,10,19]. In this case, the mean time the particle reaches a fixed target is finite (without restart, it diverges in an unbounded domain). Further, the mean time to reach a target has a distinct minimum and, thus, optimal value, as a function of t_r [9–11,16,60]. In contrast, using quantum walks, we will find several minima, instead of a unique minimum, and the mean FDPT can exhibit a bistable behavior where the hitting time is optimal for a pair of values of t_r.

Consider a classical random walk on the integers, and let $P^{\rm cl}(x,t)$ be the probability of finding the particle on x at time t. The master equation is [1]

$$\partial_t P^{\rm cl}(x,t) = \gamma[P^{\rm cl}(x+1,t) + P^{\rm cl}(x-1,t) - 2P^{\rm cl}(x,t)]. \quad (1)$$

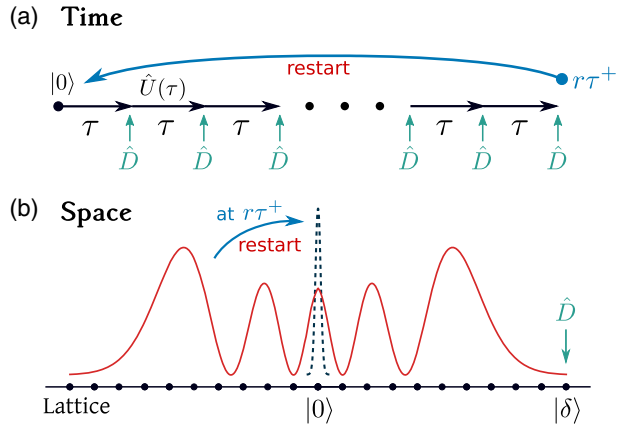

FIG. 1. The measurement protocol under sharp restart in time (a) and space (b) representation. The system is initialized at state $|0\rangle$ [see, also, the dashed needle in (b)] and the unitary evolution $\hat{U}(\tau)$ is repeatedly interrupted by projective measurements defined with $\hat{D} = |\delta\rangle\langle\delta|$ at times $\tau, 2\tau, 3\tau, \ldots$. If the state is detected, we are done, if not, at the rth failure of detection, the system is brought back to $|0\rangle$, i.e., a restart is performed every r steps. The red curve in (b) represents the wave packet, namely, the solution of Eq. (2), that spreads out ballistically before the particle is detected or reset.

γ is the hopping rate. Now, consider the tight-binding quantum walk, the wave-function is $|\psi(t)\rangle = \sum_{-\infty}^{\infty} \phi(x,t)|x\rangle$ and using the Schrödinger equation

$$-i\partial_t \phi(x,t) = \gamma[\phi(x+1,t) + \phi(x-1,t) - 2\phi(x,t)], \quad (2)$$

with $\hbar = 1$. In both models, the walker hops to nearest neighbors and the solutions for starting from the origin $|x\rangle = |0\rangle$ are $\phi(x,t) = i^x e^{-i2\gamma t} J_x(2\gamma t)$ [54], $P^{\mathrm{cl}}(x,t) = i^{-x} e^{-2\gamma t} J_x(i2\gamma t)$ [1], where $J_\alpha(z)$ is the Bessel function of the first kind. Replacing t with it one may switch from $P^{\mathrm{cl}}(x,t)$ to $\phi(x,t)$. Still, the packet spreadings are different: the classical packet spreads diffusively and approaches a Gaussian for large times, while the quantum walk propagates ballistically [39].

Quantum systems generally lack precise trajectories. Hence, to define first-hitting time, we add repeated monitoring at $|\delta\rangle$, with the goal to detect the particle at this state. For that, an observer makes repeated measurements at times $\tau, 2\tau, \ldots$. Each measurement is a projection, namely, either the particle is found at $|\delta\rangle$ (yes), or it is not (no), see Fig. 1. This yields a string of measurements, no, no, …, and in the nth attempt, a yes [50,52,54]. The process of search is then completed. Clearly, the first time we get a click yes is random, and $n\tau$ is defined as the hitting time or the FDPT. Note that, classically, the continuous sampling of the process $\tau \to 0$ makes sense, but with the quantum framework, this leads to a freeze of the dynamics and to null detection due to the quantum Zeno effect [61].

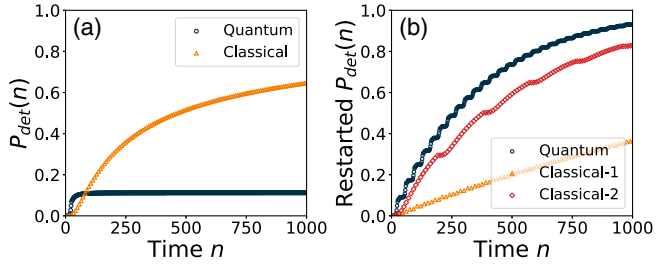

FIG. 2. (a) Detection probability $P_{\mathrm{det}}(n)$ for a classical or quantum walker on an infinite 1D lattice. The quantum total detection probability $P_{\mathrm{det}} = \sum_{n=1}^{\infty} F_n \approx 0.1$, although it grows rapidly at the beginning. The figure illustrated that for short times, the quantum ballistic spreading speeds up the search (compared to the classical counterpart), but at long times, the quantum detection without restart performs poorly. (b) Restarted quantum walk performs by far better than the corresponding classical walk, when $r = 35$ for both models (classical 1). The quantum restart process also performs better if compared with the optimally chosen classical restart (classical 2 when $r = 191$). Here, $\tau = 0.25$, $\delta = 10$.

Let F_n be the probability of detecting the walker in the nth attempt for the first time without restart. Classical and quantum renewal equations were extensively used to obtain these basic probabilities [1,54]. The quantum F_n's are presented in Table I, see, also, details below and the Supplemental Material (SM) [62]. To start, we plot, in Fig. 2(a), the detection probability up to time $n\tau$, i.e., $P_{\mathrm{det}}(n) = \sum_{n'=1}^{n} F_{n'}$ still without restart (with $\gamma = 1$). We see that, at short times $n\tau$, the quantum walker is performing better, as it has the advantage of ballistic propagation. However, at large times, the classical walker wins in the sense that it is eventually detected with probability one while the quantum system falls far from this limit [55].

To improve the hitting time, we use the sharp-restart strategy [7,16], leaving other cases to the SM [62], see, also, further discussion at the end of the Letter. Every r detection attempts we restart the search process, as Fig. 1 depicts. With this approach, we find both simple and novel results, we start with the former. Using the simple example in Fig. 2(a), if we choose r to be slightly larger than the time it takes the quantum $P_{\mathrm{det}}(n)$ to saturate without restart, we observe two effects presented in Fig. 2(b). First, the quantum detection is now guaranteed: with probability one, we detect the walker in the long time limit (the same

TABLE I. F_n for the model of an infinite line, $\delta = 0$.

n	F_n
1	$\lvert J_0(2\gamma\tau)\rvert^2$
2	$\lvert J_0(4\gamma\tau) - J_0^2(2\gamma\tau)\rvert^2$
3	$\lvert J_0^3(2\gamma\tau) - 2J_0(4\gamma\tau)J_0(2\gamma\tau) + J_0(6\gamma\tau)\rvert^2$
4	$\lvert -J_0^4(2\gamma\tau) + 3J_0(4\gamma\tau)J_0^2(2\gamma\tau) - 2J_0(6\gamma\tau)J_0(2\gamma\tau) - J_0^2(4\gamma\tau) + J_0(8\gamma\tau)\rvert^2$

for the classical cases). Second, the quantum walker performs much better than the classical one (classical 1), in the sense of a much larger quantum $P_{\rm det}(n)$ compared with the classical case. If r is chosen as the optimal for the classical walk to make a fair comparison, the quantum restart process still performs better than the classical one (classical 2). This is obviously due to the quantum ballistic propagation.

To gain insight, we will focus on the expected FDPT under restart, denoted by $\langle t_f\rangle_r$. By definition $\langle t_f\rangle_r = \tau\langle n_f\rangle_r = \tau(r\langle\mathcal{R}\rangle + \langle\tilde{n}\rangle)$, where n_f is the number of measurements until first hitting, $\mathcal{R}$ is the number of restarts before final detection. Hence, $0 \le \mathcal{R} \le \infty$ and $1 \le \tilde{n} \le r$. The joint distribution of $\mathcal{R}$ and $\tilde{n}$ is $\Pr_r(\mathcal{R},\tilde{n}) = [1-P_{\rm det}(r)]^{\mathcal{R}}F_{\tilde{n}}$, with the normalization $\sum_{\mathcal{R}=0}^{\infty}\sum_{\tilde{n}=1}^{r}\Pr_r(\mathcal{R},\tilde{n}) = 1$. Using the restart time $t_r = r\tau$, we obtain [7,30,63]

$$\langle t_f\rangle_r = \underbrace{\frac{1-P_{\rm det}(r)}{P_{\rm det}(r)}}_{\langle\mathcal{R}\rangle t_r} t_r + \underbrace{\sum_{\tilde{n}=1}^{r}\frac{(\tilde{n}\tau)F_{\tilde{n}}}{P_{\rm det}(r)}}_{\tau\langle\tilde{n}\rangle}, \tag{3}$$

(see SM [62] for detailed derivation). In turn, the probabilities F_n were studied previously in Refs. [54,55] and, as mentioned for small n, are presented in Table I (for $\delta = 0$). The F_n's are used to evaluate observables of interest numerically, though clearly as a stand-alone quantity, they do not provide much insight. Now, we focus on the optimization for $\langle t_f\rangle_r$ in small and large τ limits where applicable approximations allow analytical solutions.

Zeno limit.—Now, we consider the case where τ is small, and hence, the measurements are frequent. Let $g(t_f)dt_f$ be the probability of t_f, in the absence of restart, to be in the interval $[t_f, t_f + dt_f]$. In this limit, the process can be modeled with a continuous time formalism, which is a great simplification [52,57]. This means that we can treat $g(t_f) = \sum_{n=1} F_n\delta(t_f - n\tau)$ as a smooth function. The main tool here is a non-Hermitian Schrödinger equation, $i|\dot{\Psi}\rangle = [H - i\hbar(2/\tau)|\delta\rangle\langle\delta|]|\Psi\rangle$, and $S(t) = \langle\Psi(t)|\Psi(t)\rangle$ is the probability that the walker "survived" from detection until time t, and $g(t_f) = -dS(t)/dt|_{t=t_f}$. With this approach and H defined in Eq. (2), one finds that, without restart [56,64],

$$g(t_f) = \tau\delta^2\frac{J_\delta^2(2t_f)}{t_f^2}. \tag{4}$$

As $\tau \to 0$, this expression exhibits the well-known Zeno physics, i.e., frequent measurement prohibits state transitions [61]. To remedy this problem we use restart.

Using Eq. (3) in the continuous limit yields

$$\langle t_f\rangle_r \sim [(\delta^2\tau\mathcal{I}_1)^{-1} - 1]t_r + \mathcal{I}_2/\mathcal{I}_1, \tag{5}$$

where $\mathcal{I}_1 = \int_0^{t_r} t_f^{-2}J_\delta^2(2t_f)dt_f$, $\mathcal{I}_2 = \int_0^{t_r} t_f^{-1}J_\delta^2(2t_f)dt_f$ (see SM [62] for explicit solutions). The theory Eq. (5) nicely matches numerical results obtained from the repeated-measurement model (see SM [62]). In Fig. 3, we present $\langle t_f\rangle_r$ as a function of t_r, on top of which the global minimum of $\langle t_f\rangle_r$ (red dots) is provided via minimization of Eq. (5), which remarkably is τ (δ) independent (dependent), respectively. Soon, we will explain this intriguing feature.

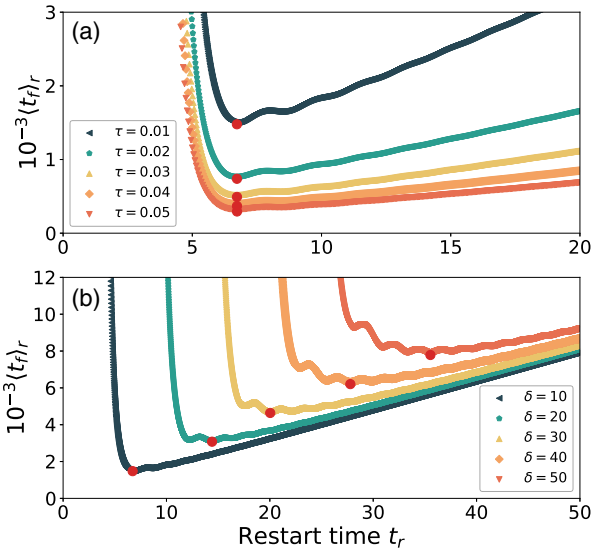

FIG. 3. $\langle t_f\rangle_r$ vs restart time t_r for different δ and τ, obtained using the repeated-measurement model. The red dots are the minimum calculated using the non-Hermitian approximation Eq. (5). Notice the oscillations which are a quantum feature. We used $\delta = 10$ (a), and $\tau = 0.01$ (b). The optimal restart time is τ independent (a) while exhibiting a nearly linear dependence on the distance δ (b).

We also see, in Fig. 3, that for too small or too large t_r, the mean hitting time diverges as expected. Specifically, using Eq. (5), for $\delta \neq 0$, $\langle t_f\rangle_r \sim (2\delta-1)\Gamma^2(1+\delta)t_r^{2(1-\delta)}/\tau\delta^2$ when $t_r \to 0$, and $\langle t_f\rangle_r \sim [\pi(4\delta^2-1)/8\tau\delta^2 - 1]t_r + (4\delta^2-1)\pi/16\delta$ as $t_r \to \infty$. Hence, for large t_r and large δ, $\langle t_f\rangle_r$ is linear in t_r with a δ-independent slope, which is vastly different from the classical behavior, as the latter is proportional to δ [9].

The detection time under restart features oscillations, clearly visible in Fig. 3. These oscillations are, in turn, related to the phase acquired in $g(t_f) \sim (\delta^2\tau/\pi)t_f^{-3}\cos^2(2t_f - \pi\delta/2 - \pi/4)$ in large t_f limit of Eq. (4). The quantum oscillations presented in Fig. 3 imply that we have, in general, multiple extrema for $\langle t_f\rangle_r$, instead of a unique minimum usually found for classical restarts [9–11,16,60], see, also, SM [62] where we present classical examples. Using Eq. (5), the extrema are solutions to

$$\tau\xi - \tau^2\left[\xi\int_0^{t_r^{\rm ext}}\tilde{g}(t)dt + \int_0^{t_r^{\rm ext}}t\tilde{g}(t)dt\right] = 0, \tag{6}$$

where $\tilde{g}(t) = g(t)/\tau$, $\xi = \int_0^{t_r^{\rm ext}} \tilde{g}(t)dt - t_r^{\rm ext}\tilde{g}(t_r^{\rm ext})$, and the superscript ext means extremum. Since τ is small, we may neglect the τ^2 terms and find a transcendental equation for the extrema, i.e., $\xi = 0$ or

$$\int_0^{t_r^{\rm ext}} \frac{J_\delta^2(2t)}{t^2}dt = \frac{J_\delta^2(2t_r^{\rm ext})}{t_r^{\rm ext}}, \tag{7}$$

(see SM [62] for an explicit solution to the integral). Hence, the extrema are independent of τ, as demonstrated in Fig. 3. Note that a similar technique to derive the optimum is also used from classical walks [19, Eq. (7)]. Remarkably, since, as mentioned after Eq. (2), $|J_\delta(2t)|^2$ is the probability of finding the walker at $|\delta\rangle$, in the absence of measurements, the extremal restart times are actually connected to the solution of the Schrödinger equation $|\phi(\delta, t)|^2$. The transcendental Eq. (7) indicates that the number of extrema increases as δ grows. Unlike the classical problem, the global minimum t_r^* increases roughly linearly with the distance δ and exhibits sudden jumps at special δ's due to the multiple minima (see SM [62]).

Large τ limit.—Also, when the measurement period τ is large, we find interesting effects. In this case, and without restart, the probability of FDPT F_n is given by the wave function of the system in the absence of measurements. The origin of this effect is that sparse measurements do not modify the Hermitian dynamics too much. Specifically, using the asymptotics of the Bessel function [54,65]

$$F_n(\tau) = |\langle 0|\psi(t = n\tau)\rangle|^2 \sim \frac{1}{n\pi\tau}\cos^2\left(2n\tau - \frac{\pi}{4}\right). \tag{8}$$

Here, we have focused on the case called the return problem when $\delta = 0$, partly due to space limitation. In Fig. 4, we plot $r^* = t_r^*/\tau$ vs τ using a numerically exact calculation. Clearly, unlike the Zeno case, now τ is an important parameter. Remarkably, as shown in Fig. 4, r^* exhibits a periodic sequence of staircases, which are now analyzed.

Beyond the fact we get for the optimum r^* periodiclike behavior, there are plunges for certain critical τ's in Fig. 4. This means that the optimal restart step jumps from $r^* = 6$ to $r^* = 1$, when τ is only slightly modified. This indicates the existence of instabilities in the system, related to quantum oscillations. To understand these effects, we used Eq. (8). First, notice that choosing 2τ as a multiple of π, we have $F_n \sim 1/(2n\pi\tau)$. Since F_n is monotonically decaying with n, it is not difficult to realize that the optimal strategy to restart is to choose $r^* = 1$, namely, immediate restart (this holds in the classical counterpart since the first-passage probability decays as $t^{-3/2}$ [1]). This explains the periodicity presented in Fig. 4. As we vary τ, then close to $\tau = k\pi/2$ with k a positive integer, the best strategy is to restart as fast as possible, i.e., $r^* = 1$.

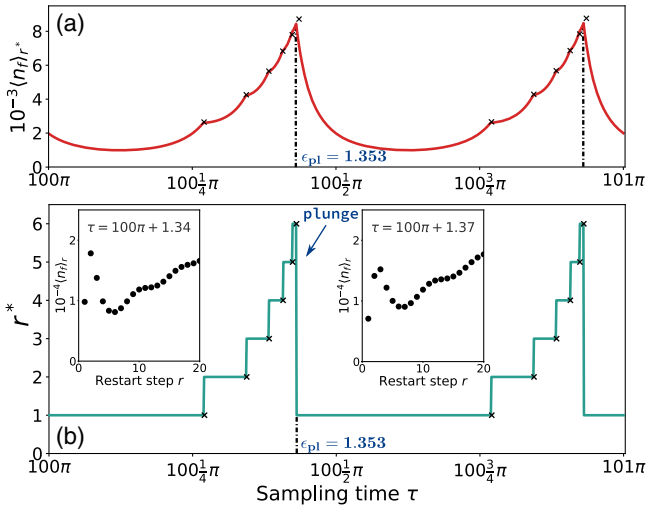

FIG. 4. (a) $\langle n_f\rangle_{r^*}$ vs τ. $\langle n_f\rangle_{r^*} \sim 1/F_{r^*+1}$ is used to calculate the theoretical optima at transition points (black crosses), around which nonsmoothness is witnessed. (b) The optimal restart step r^* vs τ. We see the novel staircase structure in large τ, however, this type of behavior appears in the full range of τ (see SM [62]). The black crosses represent the theoretical transition τ's Eq. (10). For classical restart, $r^* = 1$. The insets present $\langle n_f\rangle_r$ vs r in the vicinity of the plunge τ ($= 100\pi + 1.353$). There are two minima competing with each other, and a small change of τ (i.e., $\Delta\tau = 0.03$) results in different optima. On the left inset, $r^* = 6$, and on the right, $r^* = 1$. We used $\delta = 0$.

What will happen when we increase τ? Considering the mean $\langle n_f\rangle_r = \langle t_f\rangle_r/\tau$, note that $\langle n_f\rangle_1 = 1/F_1$, and importantly, when τ is large such that $F_n \ll 1$, we have $\langle n_f\rangle_2 \sim 2/(F_1 + F_2)$, $\langle n_f\rangle_3 \sim 3/(F_1 + F_2 + F_3)$, etc. Let $\tau = k\pi/2 + \epsilon$ and $0 < \epsilon < \pi/2$. As mentioned for $\epsilon = 0$, $r^* = 1$. When the condition $\langle n_f\rangle_1 = \langle n_f\rangle_2$ holds, there is a transition from $r^* = 1$ to $r^* = 2$ taking place when $\epsilon_{1\to 2} = 0.850$ (see derivation in SM [62]). Further transitions in r^* from r to $r + 1$ take place whenever

$$rF_{r+1} = \sum_{n=1}^{r} F_n. \tag{9}$$

Importantly, this formula admits a finite number of solutions, which based on physical intuition, is expected since r^* cannot be too large. Using Eqs. (8), (9) we find those $\epsilon_{j\to j+1}$ on which the steplike jumps take place, with j increasing from 1 to 5,

$$\{\epsilon_{j\to j+1}\} = \{0.850, 1.081, 1.204, 1.280, 1.332\},$$
$$\epsilon_{\rm pl} = 1.353. \tag{10}$$

The subscript pl means plunge, i.e., the jump from $r^* = 6$ to $r^* = 1$. Thus, as shown in Fig. 4, we have a complete theory of the staircase structure. Further, using the smallness of F_n, we have, at transition points, $\langle n_f\rangle_{r^*} \sim 1/F_{r^*+1}$.

To better understand the "plunge" namely the transition $r^* = 6 \to r^* = 1$ found for $\epsilon_{\rm pl}$, $\langle n_f \rangle_r$ close to a critical value of τ is plotted in the insets of Fig. 4. There appear two minima of $\langle n_f \rangle_r$. The first is at $r^* = 6$ and the second at $r^* = 1$. A slight change of τ leads to the global minimum switching from one value to the other. At the exact transition value, the two minima are identical. Thus, the system exhibits an instability in the sense that small changes of τ create a large difference in r^*.

Discussion.—Employing the sharp-restart strategy, we expedite the hitting time of a tight-binding quantum walk, and now, we emphasize three points. First, the expected hitting time under restart exhibits an oscillatory behavior unlike the classical case, rendering the appearance of several extrema. This effect is general and not limited to the Zeno limit, as we will show in a future publication. What is unique to this limit, is that the optimal restart is τ independent, and that one may obtain a transcendental equation which is a by far simpler tool if compared with an exact though numerical evaluation of the problem. Second, previously, it was shown that sharp restart has a certain advantage of attaining the lowest mean passage time among all restart strategies [7,16]. It is also noteworthy that the quantum feature of oscillations is wiped out with Poisson or geometric restarts (see details in SM [62]), thus, sharp restart should be used in the quantum domain. Third, in sparse measurement limit, i.e., large τ, the optimal restart step r^* exhibits a periodical staircase structure with instabilities, i.e., plunges in the optimal restart time (Fig. 4). We expect these instabilities to be generic for a wide range of parameter changes, as their cause is the oscillatory nature of the detection time statistics. These plunges and instabilities are clearly a signature of the quantum dynamics, and as far as we know, are new in the general framework of restart theory.

Our theory can be implemented in laboratories, as restarts are routinely used, for the aim of repeating experimental protocols to gain statistics of various outputs. Probably the best way to test the theory is on quantum computers. Here, the repeated strong measurements needed for hitting time statistics and the restarts, i.e., the returning of the system to its initial state, are now built in parts of the quantum computing package. The quantum walk part is implemented by the Jordan-Wigner transformation that maps the walk to a qubit representation [59]. It should be noted that system size does not have to be large, as some of the effects we found here, like staircases and plunges (Fig. 4), are generic to all quantum systems.

The support of Israel Science Foundation's Grant No. 1614/21 is acknowledged.

[1] S. Redner, *A Guide to First-Passage Processes* (Cambridge University Press, Cambridge, England, 2001).
[2] R. Metzler, G. Oshanin, and S. Redner, *First-Passage Phenomena and Their Applications* (World Scientific, Singapore, 2014).
[3] B. Munsky, I. Nemenman, and G. Bel, J. Chem. Phys. **131**, 235103 (2009).
[4] G. Bel, B. Munsky, and I. Nemenman, Phys. Biol. **7**, 016003 (2009).
[5] S. Reuveni, M. Urbakh, and J. Klafter, Proc. Natl. Acad. Sci. U.S.A. **111**, 4391 (2014).
[6] T. Rotbart, S. Reuveni, and M. Urbakh, Phys. Rev. E **92**, 060101(R) (2015).
[7] M. Luby, A. Sinclair, and D. Zuckerman, *[1993] The 2nd Israel Symposium on Theory and Computing Systems* (IEEE, Natanya, Israel, 1993), 128.
[8] C. P. Gomes, B. Selman, and H. A. Kautz, in *Proceedings of the Fifteenth National/Tenth Conference on Artificial Intelligence/Innovative Applications of Artificial Intelligence* (American Association for Artificial Intelligence, Madison, Wisconsin, USA, 1998).
[9] M. R. Evans and S. N. Majumdar, Phys. Rev. Lett. **106**, 160601 (2011).
[10] M. R. Evans and S. N. Majumdar, J. Phys. A **44**, 435001 (2011).
[11] M. R. Evans and S. N. Majumdar, J. Phys. A **47**, 285001 (2014).
[12] D. Boyer and C. Solis-Salas, Phys. Rev. Lett. **112**, 240601 (2014).
[13] S. Gupta, S. N. Majumdar, and G. Schehr, Phys. Rev. Lett. **112**, 220601 (2014).
[14] S. Eule and J. J. Metzger, New J. Phys. **18**, 033006 (2016).
[15] S. Reuveni, Phys. Rev. Lett. **116**, 170601 (2016).
[16] A. Pal and S. Reuveni, Phys. Rev. Lett. **118**, 030603 (2017).
[17] A. Falcón-Cortés, D. Boyer, L. Giuggioli, and S. N. Majumdar, Phys. Rev. Lett. **119**, 140603 (2017).
[18] S. Belan, Phys. Rev. Lett. **120**, 080601 (2018).
[19] A. Chechkin and I. M. Sokolov, Phys. Rev. Lett. **121**, 050601 (2018).
[20] M. R. Evans and S. N. Majumdar, J. Phys. A **51**, 475003 (2018).
[21] D. Boyer, A. Falcón-Cortés, L. Giuggioli, and S. N. Majumdar, J. Stat. Mech. (2019) 053204.
[22] A. S. Bodrova, A. V. Chechkin, and I. M. Sokolov, Phys. Rev. E **100**, 012120 (2019).
[23] A. S. Bodrova, A. V. Chechkin, and I. M. Sokolov, Phys. Rev. E **100**, 012119 (2019).
[24] L. Kuśmierz and E. Gudowska-Nowak, Phys. Rev. E **99**, 052116 (2019).
[25] B. Besga, A. Bovon, A. Petrosyan, S. N. Majumdar, and S. Ciliberto, Phys. Rev. Res. **2**, 032029(R) (2020).
[26] M. Magoni, S. N. Majumdar, and G. Schehr, Phys. Rev. Res. **2**, 033182 (2020).
[27] M. R. Evans, S. N. Majumdar, and G. Schehr, J. Phys. A **53**, 193001 (2020).
[28] B. De Bruyne, J. Randon-Furling, and S. Redner, Phys. Rev. Lett. **125**, 050602 (2020).
[29] O. Tal-Friedman, A. Pal, A. Sekhon, S. Reuveni, and Y. Roichman, J. Phys. Chem. Lett. **11**, 7350 (2020).
[30] I. Eliazar and S. Reuveni, J. Phys. A **54**, 125001 (2021).

[31] B. D. Bruyne, J. Randon-Furling, and S. Redner, J. Stat. Mech. (2021) 013203.
[32] V. Méndez, A. Masó-Puigdellosas, T. Sandev, and D. Campos, Phys. Rev. E **103**, 022103 (2021).
[33] S. N. Majumdar, F. Mori, H. Schawe, and G. Schehr, Phys. Rev. E **103**, 022135 (2021).
[34] M. Dahlenburg, A. V. Chechkin, R. Schumer, and R. Metzler, Phys. Rev. E **103**, 052123 (2021).
[35] R. K. Singh, T. Sandev, A. Iomin, and R. Metzler, arXiv: 2105.08112.
[36] Y. Aharonov, L. Davidovich, and N. Zagury, Phys. Rev. A **48**, 1687 (1993).
[37] E. Farhi and S. Gutmann, Phys. Rev. A **58**, 915 (1998).
[38] J. Kempe, Contemp. Phys. **44**, 307 (2003).
[39] Y. Lahini, A. Avidan, F. Pozzi, M. Sorel, R. Morandotti, D. N. Christodoulides, and Y. Silberberg, Phys. Rev. Lett. **100**, 013906 (2008).
[40] O. Mülken and A. Blumen, Phys. Rep. **502**, 37 (2011).
[41] B. Mukherjee, K. Sengupta, and S. N. Majumdar, Phys. Rev. B **98**, 104309 (2018).
[42] D. C. Rose, H. Touchette, I. Lesanovsky, and J. P. Garrahan, Phys. Rev. E **98**, 022129 (2018).
[43] S. Belan and V. Parfenyev, New J. Phys. **22**, 073065 (2020).
[44] G. Perfetto, F. Carollo, M. Magoni, and I. Lesanovsky, Phys. Rev. B **104**, L180302 (2021).
[45] G. Perfetto, F. Carollo, and I. Lesanovsky, SciPost Phys. **13**, 079 (2022).
[46] X. Turkeshi, M. Dalmonte, R. Fazio, and M. Schirò, Phys. Rev. B **105**, L241114 (2022).
[47] M. Magoni, F. Carollo, G. Perfetto, and I. Lesanovsky, Phys. Rev. A **106**, 052210 (2022).
[48] F. Caruso, A. W. Chin, A. Datta, S. F. Huelga, and M. B. Plenio, J. Chem. Phys. **131**, 105106 (2009).
[49] F. Thiel, I. Mualem, D. Meidan, E. Barkai, and D. A. Kessler, Phys. Rev. Res. **2**, 043107 (2020).
[50] H. Krovi and T. A. Brun, Phys. Rev. A **74**, 042334 (2006).
[51] F. A. Grünbaum, L. Velázquez, A. H. Werner, and R. F. Werner, Commun. Math. Phys. **320**, 543 (2013).
[52] S. Dhar, S. Dasgupta, A. Dhar, and D. Sen, Phys. Rev. A **91**, 062115 (2015).
[53] S. Dhar, S. Dasgupta, and A. Dhar, J. Phys. A **48**, 115304 (2015).
[54] H. Friedman, D. A. Kessler, and E. Barkai, Phys. Rev. E **95**, 032141 (2017).
[55] F. Thiel, E. Barkai, and D. A. Kessler, Phys. Rev. Lett. **120**, 040502 (2018).
[56] F. Thiel and D. A. Kessler, Phys. Rev. A **102**, 012218 (2020).
[57] V. Dubey, C. Bernardin, and A. Dhar, Phys. Rev. A **103**, 032221 (2021).
[58] D. Das and S. Gupta, J. Stat. Mech. (2022) 033212.
[59] S. Tornow and K. Ziegler, arXiv:2210.09941.
[60] S. Gupta and A. M. Jayannavar, Front. Phys. **10**, 789097 (2022).
[61] B. Misra and E. C. G. Sudarshan, J. Math. Phys. (N.Y.) **18**, 756 (1977).
[62] See Supplemental Material at http://link.aps.org/supplemental/10.1103/PhysRevLett.130.050802 for further details, which include Poisson restart and classical examples.
[63] O. L. Bonomo and A. Pal, Phys. Rev. E **103**, 052129 (2021).
[64] P. L. Krapivsky, J. M. Luck, and K. Mallick, J. Stat. Phys. **154**, 1430 (2014).
[65] Eq. (8) is valid for not too large n, however, since our main results focus on finite r restart, the approximation Eq. (8) holds.